World Academy of Science, Engineering and Technology
International Journal of Electronics and Communication Engineering
Vol:7, No:8, 2013

The Impact of Self-Phase Modulation on Dispersion Compensated Mapping Multiplexing Technique (MMT)

Mohamed A. Elsherif and A. Malekmohammadi

***Abstract*—**An exploration in the competency of the optical multilevel Mapping Multiplexing Technique (MMT) system in tolerating to the impact of nonlinearities as Self Phase Modulation (SPM) during the presence of dispersion compensation methods. The existence of high energy pulses stimulates deterioration in the chirp compression process attained by SPM which introduces an upper power boundary limit. An evaluation of the post and asymmetric pre-post fiber compensation methods have been deployed on the MMT system compared with others of the same bit rate modulation formats. The MMT 40 Gb/s post compensation system has 1.4 dB enhancements to the 40 Gb/s 4-Arysystem and less than 3.9 dB penalty compared to the 40 Gb/s OOK-RZsystem. However, the optimized Pre-Post asymmetric compensation has an enhancement of 4.6 dB compared to the Post compensation MMT configuration for a 30% pre compensation dispersion.

***Keywords*—**Dispersion compensation, mapping multiplexing technique, self-phase modulation.

I. Introduction

THE distant high bit rate multiplexing techniques working in the constrained boundaries for the bandwidth length product are limited by fiber losses, Chromatic Dispersion (CD) and non linearities in fiber. As there is need for a high power pulses in long haul communication for Standard Single Mode Fiber (SSMF), an important parameter for the non linearites in fiber arise, known as Self-Phase Modulation (SPM). SPM appeared due to the dependence of the refractive index on the signal intensity which leads to an induced phase change for the pulse propagating in the fiber where a pulse broadening exist in the spectral domain. At high power levels, SSMF have a large anomalous dispersion due to Group Velocity Dispersion (GVD) of 17ps/nm/km at the 1550nm wavelength, therefore necessities emerge to compensate the envelope time domain pulse broadening which leads to a chirp at the end of the propagation distance. Diverse procedures have been employed to compensate the pulse chirp effect, as pre-chirp [1], reverse dispersion fiber (RDF) [2], or by changing the cladding and core radius of the fiber [3]. Methods which exploit the use of SPM effect in the compensation for the second and almost the third order dispersion parameters have been proved effective by using Dispersion Compensation Fiber (DCF) in pre and post compensation scenarios, although the latter have been addressed being more efficient [4], [5].

Recently multilevel mapping multiplexing technique was reported for the first time in [6] as an alternative multiplexing technique for high speed optical communication systems.

In this paper, for the first time to the best of our knowledge, we report a model and numerical study of SPM effects on the performance of MMT transmission system.

We modeled the dispersion balance and SPM effects in our transmission links referring to non-linear Schrodinger (NLS) equation. Simulation was performed in both dispersion post-compensated and combination of pre- and post-compensated transmission links. The optimum value of dispersion pre-compensation is reported in order to enhance the performance of MMT system in terms of SPM tolerance. In this paper we used PRBS 2^{10}-1 patterns.

Mohamed A. Elsherif and A. Malekmohammadi are with the University of Nottingham, 43500, Malaysia (e-mail: kecx3mal@nottingham.edu.my, aminmalek_m@ieee.org).

II. Mapping Multiplexing Technique

A. Symbols Format and Mapping Algorithm

MMT is a recent novelty multiplexing technique developed for high-speed transmission of optical fiber networks [6]. MMT symbol pattern is divided to S_z slots, where z is the slot index. Each slot symbolizes a cluster of the bits (Y_Δ) as shown in Table I. MMT symbols are represented asx_K:

$$x_K = \{x_0, x_1, x_2, x_3 \ldots., x_{k-1}\} \quad (1)$$

where K is the total number of symbols which is equal to

$$K = 2^n \quad (2)$$

where$n$ is the number of channels. The number of levels can be calculated as

$$L = \log_2 K \quad (3)$$

which was defined by the transmitted mapping multiplexing indices of

$$t(i) = \{t(0), t(1), t(2), \ldots., t(i-1)\} \quad (4)$$

equivalent to a different number of combination of bits as shown in Table I.

As shown in Fig. 1, in MMT partitioning manipulation, two slots with different amplitude levels were used to transmit the bits from different channels over the fiber. Hence,$y_0 y_1$and

y_2y_3 are assigned to bit clusters of $Y_{\Delta1}(y_0y_1 \Rightarrow Y_{\Delta1})$ and $Y_{\Delta2}(y_2y_3 \Rightarrow Y_{\Delta2})$for the slots $S_1$and S_2, respectively.

TABLE I
MMT TRANSMITTED DIFFERENT BITS SYMBOLS

Transmitted Symbol Index t(i)	*Ch1-Ch2 bits Slot (S1)* $y_0y_1 \Rightarrow Y_{\Delta1}$		*Ch3-Ch4 bits Slot (S2)* $y_2y_3 \Rightarrow Y_{\Delta2}$		*MMT Symbol* x_k
t(0)	*0*	*0*	*0*	*0*	x_0
t(1)	*0*	*0*	*0*	*1*	x_1
t(2)	*0*	*0*	*1*	*0*	x_2
t(3)	*0*	*0*	*1*	*1*	x_3
t(4)	*0*	*1*	*0*	*0*	x_4
t(5)	*0*	*1*	*0*	*1*	x_5
t(6)	*0*	*1*	*1*	*0*	x_6
t(7)	*0*	*1*	*1*	*1*	x_7
t(8)	*1*	*0*	*0*	*0*	x_8
t(9)	*1*	*0*	*0*	*1*	x_9
t(10)	*1*	*0*	*1*	*0*	x_{10}
t(11)	*1*	*0*	*1*	*1*	x_{11}
t(12)	*1*	*1*	*0*	*0*	x_{12}
t(13)	*1*	*1*	*0*	*1*	x_{13}
t(14)	*1*	*1*	*1*	*0*	x_{14}
t(15)	*1*	*1*	*1*	*1*	x_{15}

The duration of each MMT slot is defined as

$$T_{slot} = \frac{T_{symbol}}{2} \tag{5}$$

where T_{symbol} is the MMT symbol interval for the bit rate of $R = 1/T_{symbol}$.

The MMT symbol $x_k(t)$ can be represented as (8) which is constructed based upon the waveform of the first slot $x_{s_1}(t)$ as in (6) and the second slot $x_{s_2}(t)$ as in (7).

$$x_{s_1}(t_i) = \sum_{i=-\infty,..-1,1}^{1,3,..\infty} w_{s_1}\, \mathrm{x}(\mathrm{t}_i) \quad , 0 \le t_i < T_{slot} \tag{6}$$

$$x_{s_2}(t_i) = \sum_{i=-\infty,..-1,1}^{1,3,..\infty} w_{s_2}\, \mathrm{x}(\mathrm{t}_i) \quad , T_{slot} \le t_i < T_{symbol} \tag{7}$$

$$x_k(t_i) = x_{s_1}(t_i) + x_{s_2}(t_i) = \sum_{i=-\infty,..-1,1}^{1,3,..\infty} w_{s_1}\, \mathrm{x}(\mathrm{t}_i) + \sum_{i=-\infty,..-4,-2}^{0,2,..\infty} w_{s_2}\, \mathrm{x}(\mathrm{t}_i) \tag{8}$$

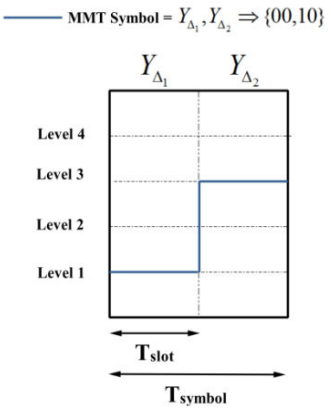

Fig. 1 MMT Symbol Format

The principle of this technique is based on a set of pre-defined mapping rules assigned in the multiplexer and de-multiplexer stages.

Fig. 2 shows different symbol structures of MMT system in a 4-channel system. 4-channel MMT has sixteen different symbols as illustrated in Fig. 2 (a). Fig. 2 (b) shows the general format of MMT symbol structure and Fig. 2 (c) represents the general eye diagram of the MMT system.

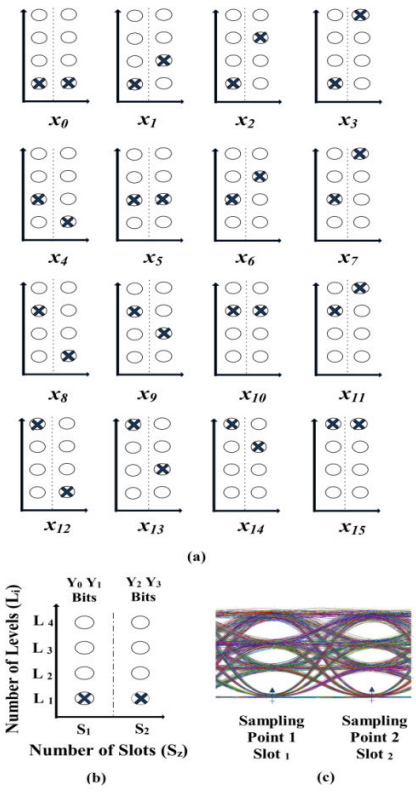

Fig. 2 (a) sixteen different symbols for a 4-channel MMT system (b) MMT Symbol Structure (c) MMT eye diagram with two sampling points

B. Data Recovery and Detection Algorithm

At the receiver side, the received signal is fed into the sampling circuit. The samples are taken at two sampling points, namely S_1 and S_2, at the first two slots in every symbol (Fig. 2 (c)). The outputs of the sampling circuit are fed into the decision and regeneration unit. In this unit, the sampled values are compared against three threshold values of, δ_1, δ_2 and δ_3.

The first slot bits represent the data for Ch_1 and Ch_2. The second slot bits represent the data for Ch_3 and Ch_4. A decoder was assigned with the corresponded transmitted symbol as shown in Fig 3.

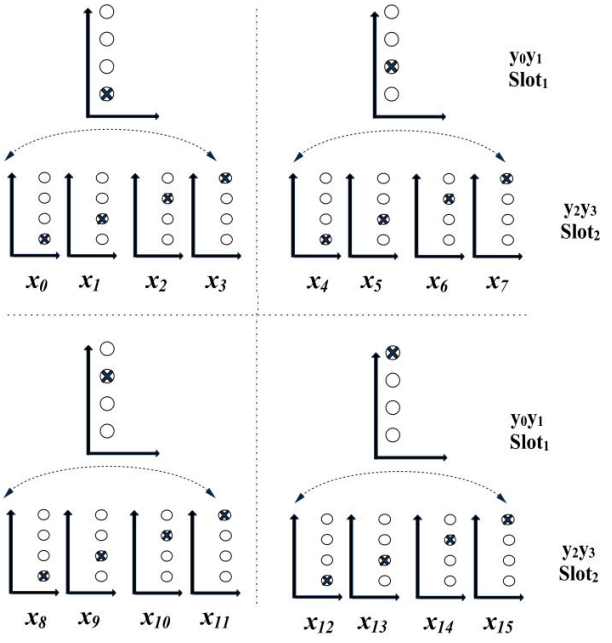

Fig. 3 Two stages decoder decision algorithm for MMT symbols.

Table II contains the regeneration rules for a MMT system that the data recovery unit uses to regenerate original data for each user. In the data recovery unit the decision can be made based on the (9), where r (k) represents the received symbol for each slot.

$$X_K = \sum_{i=1}^{i=S_z} d_{Si}(r_K) \tag{9}$$

III. Modal and Simulation

A. SPM Theoretical Modal

In this study, a hybrid system involving two softwares, MatLab and OptiSystem were used to simulate the system in both electrical and optical domain.

The mathematical model which best describes the propagation of pulse in SSMF, were taken to account for the effect of SPM and GVD in the Non Linear Schrodinger (NLS) [7] as;

$$\frac{\partial A(\tau,z)}{\partial z} = -\frac{\alpha}{2}A(\tau,z) - \frac{j}{2}\beta_2(z)\frac{\partial A(\tau,z)}{\partial \tau^2} + j\gamma\left|A(\tau,z)\right|^2 A(\tau,z) \tag{10}$$

where z is the longitudinal propagation distance, U (z,τ) is the normalized amplitude for a Gaussian pulse and the amplitude for a complex electric field pulse envelope is equal to:

$$A(z,\tau) = \sqrt{P_o}\exp(-\alpha z/2)U(z,\tau) \tag{11}$$

where $\tau = (t - z/\nu_g)/T_o$ denotes the retarded time framework for the GVD (ν_g), T_o is the pulse width , α represent the attenuation coefficient and β_2 and γ represent the GVD parameter and the fiber nonlinearity coefficient, respectively.

TABLE II
De-Mapping Detection Rules for MMT Received Symbols

Symbol Received r(k)	MMT De-Mapping Detection Rules: 1st Cluster Rule Slot 1 Ch1 - Ch2	1st Stage Decision	2nd Cluster Rule Slot 2 Ch3 - Ch4	2nd Stage Decision	Symbol Decision x_k
r(0)		$d_{S1}(r_0)$	if $S_1 < \delta_1$	$d_{S2}(r_0)$	$d_{S1}(r_0)+d_{S2}(r_0) = x_0$
r(1)		$d_{S1}(r_1)$	if $\delta_2>S_1>\delta_1$	$d_{S2}(r_1)$	$d_{S1}(r_1)+d_{S2}(r_1) = x_1$
r(2)	if $S_1< \delta_1$	$d_{S1}(r_2)$	if $\delta_3>S_1>\delta_2$	$d_{S2}(r_2)$	$d_{S1}(r_2)+d_{S2}(r_2) = x_2$
r(3)		$d_{S1}(r_3)$	if $S_1>\delta_3$	$d_{S2}(r_3)$	$d_{S1}(r_3)+d_{S2}(r_3) = x_3$
r(4)		$d_{S1}(r_4)$	if $S_1 < \delta_1$	$d_{S2}(r_4)$	$d_{S1}(r_4)+d_{S2}(r_4) = x_4$
r(5)		$d_{S1}(r_5)$	if $\delta_2>S_1>\delta_1$	$d_{S2}(r_5)$	$d_{S1}(r_5)+d_{S2}(r_5) = x_5$
r(6)	if $\delta_2>S_1>\delta_1$	$d_{S1}(r_6)$	if $\delta_3>S_1>\delta_2$	$d_{S2}(r_6)$	$d_{S1}(r_6)+d_{S2}(r_6) = x_6$
r(7)		$d_{S1}(r_7)$	if $S_1>\delta_3$	$d_{S2}(r_7)$	$d_{S1}(r_7)+d_{S2}(r_7) = x_7$
r(8)		$d_{S1}(r_8)$	if $S_1 < \delta_1$	$d_{S2}(r_8)$	$d_{S1}(r_8)+d_{S2}(r_8) = x_8$
r(9)		$d_{S1}(r_9)$	if $\delta_2>S_1>\delta_1$	$d_{S2}(r_9)$	$d_{S1}(r_9)+d_{S2}(r_9) = x_9$
r(10)	if $\delta_3>S_1>\delta_2$	$d_{S1}(r_{10})$	if $\delta_3>S_1>\delta_2$	$d_{S2}(r_{10})$	$d_{S1}(r_{10})+d_{S2}(r_{10}) = x_{10}$
r(11)		$d_{S1}(r_{11})$	if $S_1>\delta_3$	$d_{S2}(r_{11})$	$d_{S1}(r_{11})+d_{S2}(r_{11}) = x_{11}$
r(12)		$d_{S1}(r_{12})$	if $S_1 < \delta_1$	$d_{S2}(r_{12})$	$d_{S1}(r_{12})+d_{S2}(r_{12}) = x_{12}$
r(13)		$d_{S1}(r_{13})$	if $\delta_2>S_1>\delta_1$	$d_{S2}(r_{13})$	$d_{S1}(r_{13})+d_{S2}(r_{13}) = x_{13}$
r(14)	if $S_1> \delta_3$	$d_{S1}(r_{14})$	if $\delta_3>S_1>\delta_2$	$d_{S2}(r_{14})$	$d_{S1}(r_{14})+d_{S2}(r_{14}) = x_{14}$
r(15)		$d_{S1}(r_{15})$	if $S_1>\delta_3$	$d_{S2}(r_{15})$	$d_{S1}(r_{15})+d_{S2}(r_{15}) = x_{15}$

(δ_{th} represents the threshold levels)

The non-linear factor is described by the dominant parameter which is the dispersion length (L_D);

$$L_D = \frac{T_o^2}{|\beta_2|} \tag{12}$$

and the non-linear length (L_{NL}) as

$$L_{NL} = \frac{1}{\gamma P_o} \tag{13}$$

Both the GVD and SPM phenomena were considered in our system as $L \gg L_{NL}$ *and* $L \gg L_D$, where L is the fiber length.

B. 100% Post Compensation Configuration

Two simulation configurations were proposed as post dispersion compensation and pre-post dispersion compensation for a 4-channel MMT system.

Fig. 4 shows the 4-channel MMT system in a post compensation scenario. Four electrical RZ pulse carvers drive Ch_1, Ch_2, Ch_3 and Ch_4 at 10 Gbit/s per channel, which can offer an aggregated bitrate of 40 Gbit/s.

The bit stream is fed into the MMT mapping unit in order to convert the bits to the MMT symbols. The MMT symbols are used to modulate a laser diode (LD), which operates at 1550 nm wavelength using a Mach–Zehnder modulator (MZM). The optical modulator bias voltages are a key factor in the effectiveness for a receiver capability in generating an acceptable eye diagram [8]. The D-MZ modulator bias voltages have been optimized to get an optimal eye opening for MMT system.

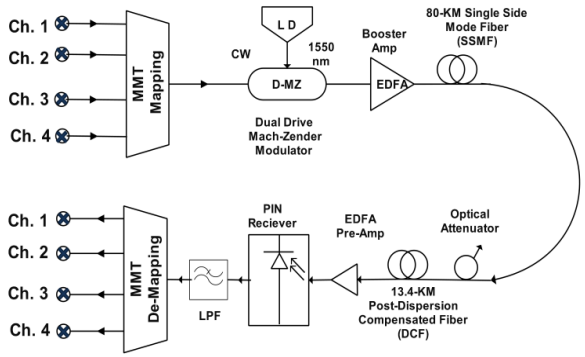

Fig. 4 Post compensation MMT configuration

The first simulation configuration was sorted for a post compensation scenario which is balanced where the total second-order dispersion system is approximately zero. Hence, the SSMF length was proposed to be 80 KM, while the DCF length was 13.4 KM. In order to inspect the effect of SPM on our actual SSMF fiber, an Erbium Doped Fiber Amplifier (EDFA) and Variable Optical Attenuators (VOA) were employed. In order to neglect the SPM effect in DCF, the launched power to the DCF was fixed to a minimum value of -13 dBm. The launched power to the SSMF was set by an in-line EDFA with Gain (G) =30 dB and noise figure of 5 dB.

The receiver consists of a PIN photodiode and a Low Pass Filter (LPF), where the symbol is then decoded to our original sent channels bit stream.

C. Pre-Post Compensation Configuration

Another optimized system configuration known as the pre-post compensation was introduced in Fig. 5 with a combination of DCF_1, SSMF and DCF_2.

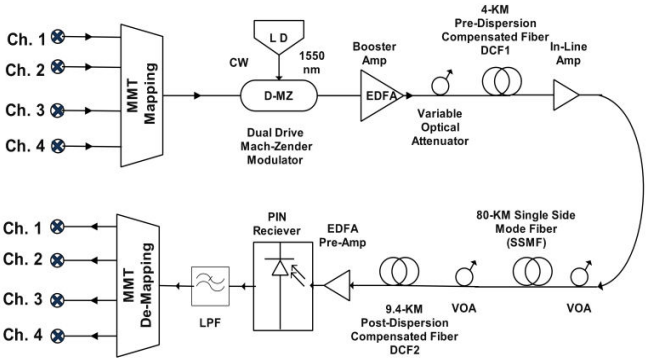

Fig. 5 The optimized pre-post compensation for MMT

TABLE III
SINGLE SIDE MODE FIBER (SSMF) SPECIFICATION

Symbol	Parameter	Value
D	Dispersion	+17 ps/nm/km
S	Dispersion Slope	0.075 ps/ nm^2/km
α	Attenuation Coefficient	0.2 dB/km
Aeff	Effective Area	80 u m^2
β_2	GVD parameter	-20 ps^2/km
n2	Non Linear Index of Refraction	26×10^{-21} m^2/W
L	SSMF Length	80 Km
DISPERSION COMPENSATED FIBER (DCF) SPECIFICATION		
D	Dispersion	-100 ps/nm/km
Aeff	Effective Area	12 u m^2

IV. RESULTS AND DISCUSSION

The initial input stream for the MMT optical input symbol sequence for the dispersion post-compensation setup was illustrated in Fig. 6 (a). While, Fig. 6 (b) shows the received symbol structure after the propagation of the optical pulses through the SSMF and before the dispersion post compensation.

It can clearly be observed from Fig. 6 (b) that several bits overlap on each other and form a non-uniform intensity distribution, which depends on the input bit stream. Owing to this, the non-linear effect is distributed unequally over different bits. Hence, when dispersion compensation is applied, different bits experience different degrees of degradation.

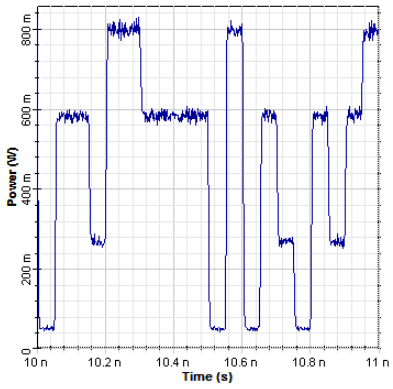

Fig. 6 (a) A portion of the optical domain transmitted MMT sequence

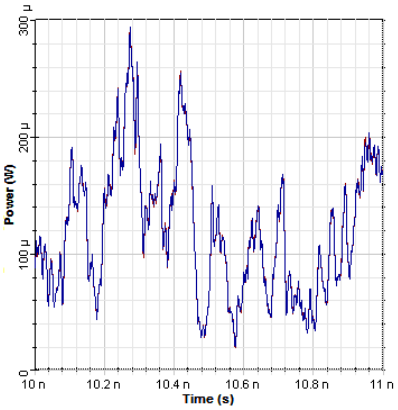

Fig. 6 (b) The received MMT sequence after SMF, before dispersion compensation

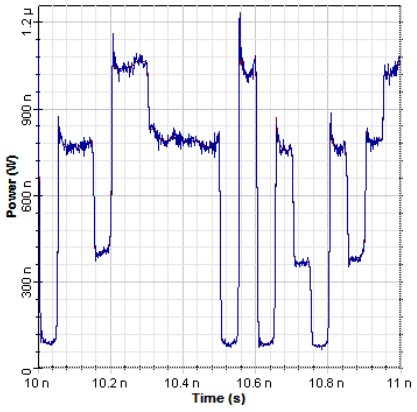

Fig. 6 (c) The received MMT sequence after dispersion post compensation

Fig. 7 illustrates an evaluative comparison of the SPM on the 40 Gbit/s MMT, 4-Ary and OOK in the 100% post compensation systems.

The minimum threshold corresponds to the power at which the Kerr non-linearity is high enough to compensate for the group velocity dispersion (GVD) limitations of the linear regime [9]. Thus the larger the residual dispersion, the higher the power needed to counterbalance its effects.

Note that a strong constraint to the minimum power threshold is also imposed by the ASE noise produced by the in-line EDFAs. This constraint, together with the power margins imposed by the SPM, especially the maximum threshold, defines the best performance region of each system.

At high powers, referring to the power at which the SPM effect take place, the signal degraded tremendously and results in higher BER. The measurements show that the maximum threshold (SPM threshold) is at BER of 10^{-9} in the MMT channel, 4-ary and OOK systems are +8.3dBm, +6.9 dBm, and 12.2 dBm, respectively. Hence, the MMT has 1.4 dB enhancements compare to the 4-ary model and less than 3.9 dB penalties compare to the OOK system.

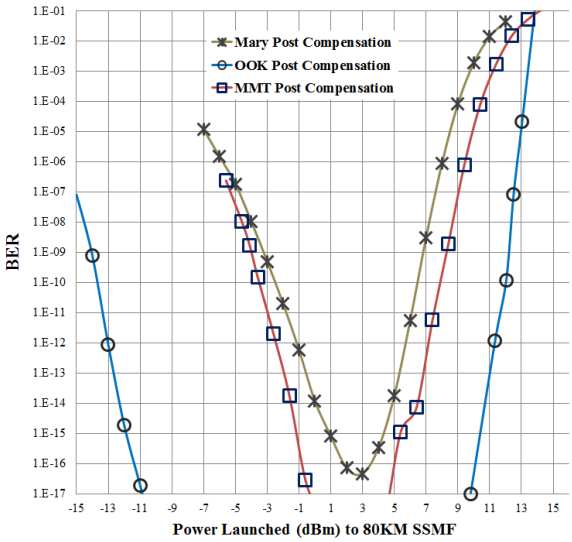

Fig. 7 SPM effect in the post-compensation setups for MMT, 4-ary and OOK systems

The impact of the SPM varies with the position of the DCF due to the nonsymmetrical distribution of GVD in the anomalous and normal regime [10]. Thus; another approach to increase the maximum SPM power threshold was introduced.

A pre-post compensation configuration was established to increase the SPM tolerance.

Fig. 8 shows a relation between the BER and the length of DCF_1 link in the case of pre-post configurations. The lunch power is fixed to +10.2 dBm. As illustrated in Fig. 8 by using 30 % pre-compensation link (equivalent to DCF_1 length of 4 KM), the BER can be improved from 10^{-2} in 100 % post-compensation (Fig. 7) to 10^{-11}.

Fig. 9 illustrates the comparison between the post and optimum combination of pre-post compensation for the fixed power of 13 dBm. The optimum combination of pre and post compensation demonstrated a remarkable enhancement of 4.6 dB in the BER.

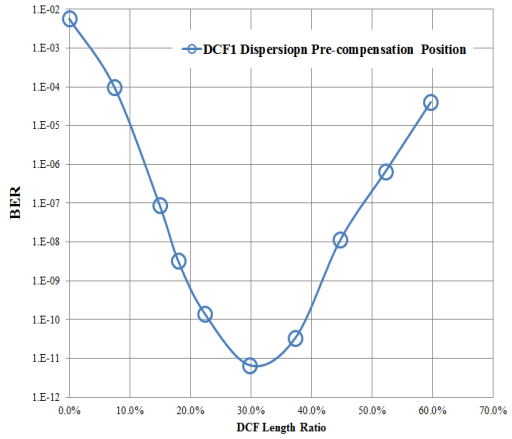

Fig. 8 Relation between the percentage of pre-compensation position and the BER with respect to the total DCF length ratio

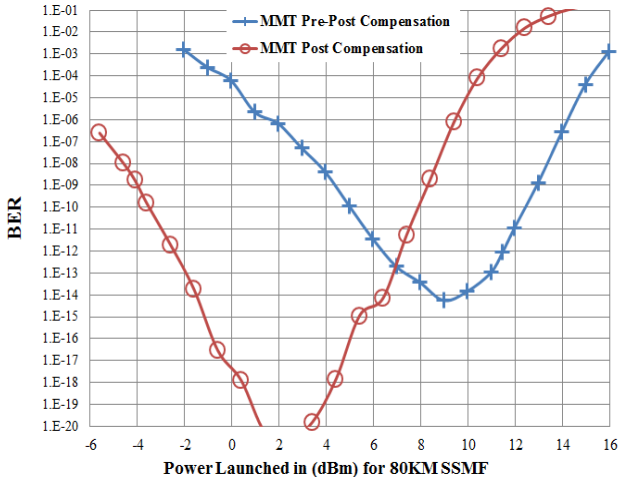

Fig. 9 BER versus lunched power

To justify the results shown in Figs. 8 and 9, Fig. 10 shows the eye diagram which is associated with +10.2dBm lunch power for (a) post compensation and (b) optimum combination of post and pre compensation.

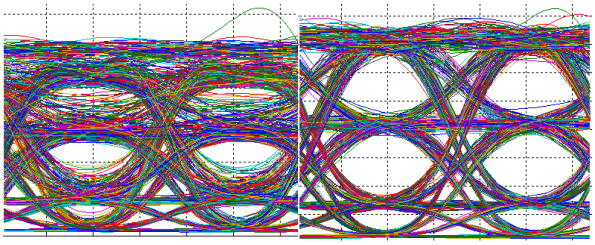

(a) (b)

Fig. 10 Eye diagram at the receiver for a launched power of 10.2 dBm (a) MMT Post-compensation configuration (b) MMT optimized Pre-Post compensation configuration

The linear eye opening penalty which leads to a higher signal distortion is correspondent with increased higher power levels as shown in Figs. 11 (a) and (b) for a launched power level of 13.1 dBm equivalent to BER of 10^{-2} and 10^{-9} for 100% post-compensation and pre-post of 30% compensation, respectively. The eye opening experienced a superposition of the symbols of each slot on each other, and an impact for the SPM increase leading to more eye closure. Hence, for increases in the signal energy, limitations on a high quality long distant transmission were conclusive.

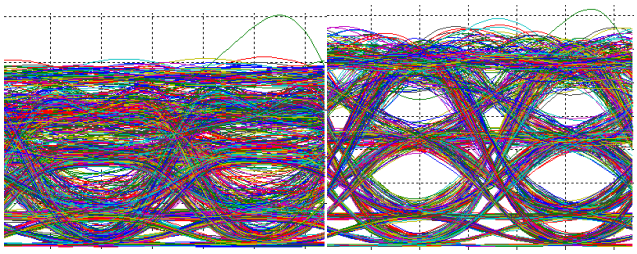

(a) (b)

Fig. 11 Eye diagram at the receiver for a launched power of 13.1 dBm after SMF (a) MMT Post-compensation configuration (b) MMT Pre-Post compensation configuration

V. Conclusion

The feasibility of the 40 Gb/s MMT as a recent mapping multiplexing technique in tolerating the effect of non linearities due to SPM phenomenon in the presence of second order dispersion parameter has been demonstrated and compared with 4-ary and RZ-OOK systems, under the effect of different dispersion compensation methods. The post-compensation MMT configuration has an advantage over 4-ary and a penalty over OOK. Nevertheless; this study introduces an optimum MMT pre-post compensation configuration which has an improved system performance and a power virtue among other dispersion compensation methods. A DCF pre-compensation length ratio dependency on the BER also has been reported in paper.

Acknowledgment

The authors would like to thank the Ministry of Science, Technology and Innovation (MOSTI) for the sponsorship of this project.

References

[1] A. H. Gnauck, S. K. Korotky, J. J. Veselka, J. Nagpal, C. T. Kemmerer, W. J. Minford and D. T. Moser, “Investigation of Pre-, Post- and Symmetric-Dispersion Compensation Techniques (DCF) using Different Modulation Formats over High-Speed Optical Link”, journal of optical communications, Volume 33, 2012.

[2] J.D. Downie, J. Hurley, M. Sauer, "Behavior of MLSE-EDC With Self-Phase Modulation Limitations and Various Dispersion Levels in 10.7-Gb/s NRZ and Duobinary Signals," Photonics Technology Letters, vol.19, no.13, pp.1017,1019, July1, 2007.

[3] T. Duthel, T.S.L. Jansen,P.M. Krummrich, M. Otto, C.G. Schaffer, "Multi-channel residual dispersion compensation in a 40 Gb/s WDM system utilizing a single all-fiber delay line filter," Optical Fiber Communication Conference, 2005. Technical Digest. OFC/NFOEC, vol.3, no., pp.3 pp. Vol. 3,, 6-11 March 2005

[4] S. Shen, C. Chang, H. P. Sardesai, V. Binjrajka, and A. M. Weiner, “Effects of self-phase modulation on sub-500 fs pulse transmission overdispersion compensated fiber links,” J. Lightw. Technol., vol. 17, no. 3, pp. 452–461, Mar. 1999.

[5] M. Schiess, "Comparison of dispersion compensation schemes includingfiber nonlinearities," J. Opt. Commun., vol. 16, no. 3, pp. 92–98,Jun. 1995.
[6] A. Malekmhammadi, M.K. Abdullah, M. Saqlain and U. Illahi, 2012. "A Novel Mapping Multiplexing Technique for High Speed Optical Fiber communication systems"*In:* 3rd International IEEE Conference on Photonics 2012 - ICP2012.
[7] Agrawal G.V.: 'Nonlinear fiber optics' (Academic Press,1999, 3rd edn., 2001), p. 35.
[8] J.C. Cartledge, "Combining self-phase modulation and optimum modulation conditions to improve the performance of 10-Gb/s transmission systems using MQW Mach-Zehnder modulators," Journal of Lightwave Technology, vol.18, no.5, pp.647,655, 2000.
[9] J.P. Gordon, "Dispersive perturbations of solitons of thenonlinear Schrodinger equation', J. Opt. Soc. Am. B, 1992, 9,pp. 91–97.
[10] J. Toulouse, "Optical nonlinearities in fibers: review, recent examples, and systems applications," Lightwave Technology, Journal of , vol.23, no.11, pp.3625,3641, Nov. 2005.